

# Hyperthermia Efficacy of PEGylated-PLGA Coated Monodisperse Iron Oxide Nanoparticles

Fatih Senturk 

 Duzce University, Department of Biophysics, Duzce, Türkiye

## ABSTRACT

Magnetic nano hyperthermia (MNH) is a promising technique for the treatment of a variety of malignancies. This non-invasive technique employs magnetic nanoparticles and alternating magnetic fields to generate local heat at the tumor location, which activates cell death pathways. However, the efficacy of MNH is dependent on the physicochemical properties of the magnetic nanoparticles, such as size, size distribution, magnetic properties, biocompatibility, and dispersibility in the medium. In this study, it is aimed to evaluate the heating capacity of poly (lactic-co-glycolic acid)-poly (ethylene glycol) diblock copolymer (PLGA-b-PEG) coated monodisperse iron oxide nanoparticles (IONs) as an effective mediator for MNH application. For this purpose, monodisperse IONs with a narrow size distribution and a mean particle size of 8.6 nm have been synthesized via the thermal decomposition method. The resulting IONs were then coated with the PEGylated-PLGA polymer and homogeneously dispersed in the polymeric matrix, which had a clearly defined spherical shape. Additionally, the specific absorption rate (SAR), reflecting the amount of heat dissipation from the NPs to the surrounding medium, was calculated for different concentrations (10, 5, 2.5, and 1.25 mg/mL) of PEGylated-PLGA-IONs. At 5 mg/mL PEGylated-PLGA-IONs (125  $\mu\text{g}_{\text{Fe}}/\text{mL}$ ) were found to have a maximum SAR value of 313 W/g. In conclusion, the homogenous dispersion of IONs in PEGylated-PLGA matrix may be one of the critical parameters to enhance the SAR value for MNH-based cancer therapy.

### Keywords:

Magnetic nano hyperthermia, Iron oxide nanoparticles, Induction heating, SAR, PLGA, PEG, PEGylated-PLGA

## INTRODUCTION

A cancer treatment strategy known as magnetic nano hyperthermia (MNH) employs magnetic nanoparticles (MNPs) to create local heat at the tumor site under the applied alternating magnetic fields (1, 2). This non-invasive technique induces physiological changes and activates death pathways in tumor cells. In hyperthermia, mild temperature increases up to 41–43°C induce the degradation of intercellular proteins, which triggers apoptosis, whereas higher temperature increases above 45°C cause the necrosis of cancer cells (3, 4). However, due to its fewer adverse effects on healthy tissue, hyperthermia-induced apoptosis is a more favorable process of cellular death mechanism than necrosis (5, 6). On the other hand, the efficiency of MNH is determined by the physical parameters of the exposure system as well as the qualities of the magnetic nanoparticles.

Iron oxide nanoparticles (IONs) with superior

magnetic properties have been widely used in various biomedical applications (7, 8), including magnetic resonance imaging, blood-brain barrier permeability (9), and MNH agents (10). In the field of MNH, IONs are the favored agent because of their ability to serve as heat mediators when exposed to an alternating magnetic field (11). However, the performance of MNH is dependent on the physicochemical qualities of IONs. Also, these qualities include size, size distribution, magnetic properties, biocompatibility, and aggregation, which determine how IONs interact with the external magnetic fields (12). Since the physicochemical characteristics of IONs are directly determined by the manufacturing procedures, fabrication methods also have an impact on MNH performance.

Iron oxide nanoparticles can be fabricated using various techniques, including co-precipitation, thermal decomposition, sonochemical decomposition, hydrot-

### Article History:

Received: 2023/02/07

Accepted: 2023/06/12

Online: 2023/06/30

Correspondence to: Fatih Senturk, Duzce University, Department of Biophysics, Duzce, Türkiye.

E-Mail: senturkfatih52@gmail.com

Phone: +90 (380) 542 1416

Fax: +90 (380) 542 1302

This article has been checked for similarity.



This is an open access article under the CC-BY-NC licence

<http://creativecommons.org/licenses/by-nc/4.0/>

hermal reactions, electrochemical deposition, etc. (13). Among them, co-precipitation and thermal decomposition are the two most commonly used techniques. However, the co-precipitation method typically results in a wide range of particle sizes, highly agglomerated particles, and poor control of the creation of particle shapes (14). In addition, one of the major barriers to biological application is the high agglomeration of nanoparticles, which may also reduce the heating ability of IONs for hyperthermia. On the other hand, the thermal decomposition method can be used to create a highly monodisperse IONs (13). These monodisperse IONs could also be coated with biocompatible/biodegradable polymers like poly(lactic-co-glycolic acid) (PLGA) and polyethylene glycol (PEG) for biological applications. Furthermore, the presence of these polymers can improve the stability and dispersibility of IONs.

The characteristics of the polymer-coated IONs play a role in the interactions between the nanoparticles and the electromagnetic fields (EMF). However, the physical parameters of the applied external EMF, mainly its frequency, are also crucial for the different types of biological interactions (15). For instance, in our previous study, a portable radiofrequency-hyperthermia (RF-HT) system with a specific frequency of 13.56 MHz was constructed and reported (4). This particular frequency (13.56 MHz) mostly interacts with the dynamic cell membrane structures, which compose of tightly packed microdomains known as lipid rafts (16, 17). Therefore, in the next study, we investigated the permeability of an in vitro blood-brain barrier (BBB) model in relation to the effects of specific 13.56 MHz frequency either alone or in the presence of nanoparticles (9). After exposure to the 13.56 MHz, it was found that transported amounts of IONs and polymer-coated IONs on the basolateral sides increased. Thus, we concluded that the 13.56 MHz combination with membrane or nanoparticles (IONs and polymer-coated IONs) can increase BBB permeability. In a different study, we tried to improve the therapeutic efficacy of multi-functionalized nanoparticles in combination with 13.56 MHz on glioblastoma cells (10). Since the membrane interaction of this 13.56 MHz specific frequency is known (17), it has been claimed that it may enhance cellular uptake by membrane interaction as well as the hyperthermia impact.

In all of the studies discussed above, a system with a frequency of 13.56 MHz was utilized in accordance with the interaction of the biological structure (cell membrane, BBB penetration, cellular uptake, etc.). However, in this research, a commercialized induction heating system was used, which produces a magnetic field at a frequency of roughly 300 kHz and is commonly used in MNH experiments. Since the focus of this research is on the interaction between a magnetic field and materials (IONs), external frequencies around 300 kHz were selected, where this interaction is stronger for

hyperthermia. To our knowledge, there is no study in which highly monodisperse IONs were embedded in PEGylated-PLGA nanoparticles and correlated the hyperthermia efficacy of these particles with concentration-dependent specific absorption rate (SAR) values. Therefore, the aim of this study is to determine the efficacy of PEGylated-PLGA coated monodisperse IONs as a hyperthermia mediator to evaluate the potential for future research on cancer therapy.

## MATERIAL AND METHODS

### Materials

Ferric chloride hexahydrate ( $\text{FeCl}_3 \cdot 6\text{H}_2\text{O}$ ), sodium oleate, 1-octadecene, oleic acid, poly(lactic-co-glycolic acid) (PLGA) (lactide:glycolide, 50:50,  $M_w$ :30,000–60,000), poly(ethylene glycol) 2-aminoethyl ether acetic acid ( $\text{COOH-PEG-NH}_2$ ,  $M_n$ :3500), 1-ethyl-3-(3-dimethyl-aminopropyl) carbodiimide (EDC), N-hydroxysuccinimide sodium salt (NHS), hexane, methanol, ethanol, dimethyl formamide (DMF), dichloromethane (DCM), polyvinyl alcohol (PVA,  $M_w$ :30,000–70,000) and iron assay kit (MAK025) were purchased from Sigma-Aldrich (Germany).

### Fabrication of monodisperse iron oxide nanoparticles (IONs)

Monodisperse iron oxide nanoparticles (IONs) were fabricated by a thermal decomposition method (18), as also reported in our previous studies (8-10). Briefly, the thermal decomposition process involves two steps. First, synthesis of iron-oleate complexes: Iron (III) chloride hexahydrate (10.8 g) and sodium oleate (36.5 g) were dissolved in a mixture of distilled water, ethanol, and hexane (60; 80; 140 mL) and heated at 70°C for 2 h. Following the end of the reaction, the iron oleate organic layer was washed three times in a separatory funnel with distilled water. In the second step of thermal decomposition, the synthesized iron oleate (36 g) and oleic acid (5.7 g) were dissolved in 1-octadecene under nitrogen ( $\text{N}_2$ ) protection and heated to 320°C for 30 min. After cooling the final solution down to room temperature, the excess surfactants were removed by washing the magnetic NPs three times with ethanol using a neodymium magnet and centrifugation (10,000 rpm, 15 min). Finally, IONs were distributed in hexane for further use.

### Fabrication of PEGylated-PLGA polymer

Di-block polymers of PLGA and PEG ( $M_n$ : 3500) were fabricated via an EDC-NHS chemistry (19). Briefly, PLGA (50 mg) was dissolved in DMF (10 mL), followed by activated with 1.20 mM EDC and 1.17 mM NHS. After allowing the solution to react overnight, the obtained PLGA

was washed three times with ice-cold methanol to remove impurities and vacuum dried. Forty milligrams of activated PLGA were dissolved in dimethylformamide (2 mL), then added 26  $\mu\text{M}$   $\text{NH}_2\text{-PEG-COOH}$  and incubated for 12 h with magnetic stirring (100 rpm). The resulting PEGylated-PLGA copolymer was precipitated, washed three times with ice-cold methanol, collected, and dried in a vacuum prior to further use.

### Fabrication of PEGylated-PLGA coated monodisperse IONs

PEGylated-PLGA polymer coating of IONs was carried out by a single emulsion-solvent evaporation method (20). Briefly, 2 mg of IONs and 20 mg PEGylated-PLGA polymers were mixed in 4 mL DCM, forming the emulsion's organic phase. The organic phase was then added dropwise to 20 mL of 1% (w/v) PVA aqueous solution under stirring at 15,000 rpm with an ultra-turrax homogenizer for 10 min. Next, the organic solvent (DCM) was evaporated while the emulsion was mechanically stirred with a non-magnetic PTFE stirrer for 4 h at room temperature. Subsequently, the PEGylated-PLGA-IONs were washed three times by centrifugation (11,000 rpm, 30 min) to remove excess reactants. The collected PEGylated-PLGA-IONs were finally freeze-dried and stored at 4°C until further use.

### Characterization of nanoparticles

The morphology and size of the fabricated nanoparticles were investigated by field emission scanning electron microscopy (Quanta 400F SEM, USA) and transmission electron microscopy (TEM, FEI Tecnai G2 Spirit BioTwin, USA). The average size and standard deviation of the IONs and PEGylated-PLGA-IONs were calculated from more than 200 particles in electron microscope images utilizing ImageJ software. The polydispersity index (PDI) describes the particle size distribution. The PDI value may vary from 0 to 1, while the PDI value less than 0.1 implies monodisperse particles and the values more than 0.1 may indicate polydisperse particle size distributions. The formula for the polydispersity index is presented as follows (21).

$$PDI = (\sigma / d)^2 \quad (1)$$

Where  $\sigma$  represents the standard deviation and  $d$  indicates the mean particle diameter. The hysteresis loops of IONs and PEGylated-PLGA-IONs were recorded at room temperature with a physical property measurement system of Quantum Design (QD-PPMS, USA) in magnetic fields between  $-2$  to 2 Tesla.

### Magnetic heating experiments of nanoparticles

The heating ability of PEGylated-PLGA coated IONs is investigated using an induction heating system (Easy Heat 8310, Ambrell, UK) (Fig. 1a) with a 3.43 cm diameter and 8-turns coil (Fig. 1b). Heat generation was controlled at ambient temperature by running cold water through the induction coil's hollow tube. The prepared PEGylated-PLGA-IONs were dispersed in distilled water (2.5 mL) and sonicated for 2 min to improve dispersion homogeneity. Then, the suspension was placed inside the coil, and magnetic field was applied for 10 min (100 A, 312 kHz). After that, magnetic field strength ( $H$ ) was calculated using Equation (2).

$$H = 1.257 \, ni / L(Oe) \quad (2)$$

where  $i$  represents the coil's current value,  $L$  its diameter in centimeters, and  $n$  its number of turns (22). The calculated magnetic field strength was  $H = 23.51$  kA/m, and the induced temperature of the solution was recorded using a fiber optic temperature sensor (Neoptix, Canada) throughout the exposure (Fig. 1b and 1c). Afterwards, the specific absorption rate (SAR), which is the main parameter of heat dissipation of magnetic nanoparticles (23), was calculated to evaluate the heating efficiency of PEGylated-PLGA-IONs at different concentrations (10, 5, 2.5, 1.25 mg/mL). The SAR value is calculated by using the following Equation (3) (24).

$$SAR (W / g) = C (m_s / m_{Fe}) (\Delta T / \Delta t) \quad (3)$$

Where the  $C$  refers to suspension's specific heat capacity ( $C_{\text{water}} = 4.185$  J/g°C),  $m_s$  for the mass of the solution,  $m_{Fe}$  for the mass of iron (Fe), and  $\Delta T / \Delta t$  for the slope measured from the heating curves.

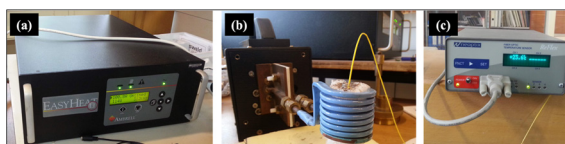


**Figure 1.** Induction heating system (Easyheat 8310, Ambrell, UK), (a) power supply, (b) induction coil (8-turns) with fiber optic temperature probe, (c) fiber optic temperature measurement system (Neoptix, Canada).

It has been noted that some researchers provide SAR results in Watts per mass of nanoparticles (W/mNPs) (25, 26), whereas others report Watts per mass of Fe (W/mFe) (27, 28). In this paper, SAR values were expressed in Watts per unit mass of iron (W/mFe). Therefore, a colorimetric approach was used to determine the iron content in PEGylated-PLGA nanoparticles with iron assay kit components. A microplate reader (Asys UVM340, Austria) was used to measure the solutions' absorbance at 593 nm in 96-well plates. Iron assay kit components were also used to create standard solutions

with known iron concentrations. Next, the iron concentration of PEGylated-PLGA-IONs was calculated using a standard calibration curve.

## RESULTS AND DISCUSSION

### Fabrication and characterization of IONs and PEGylated-PLGA coated IONs

A detailed physicochemical characterization of iron oxide nanoparticles (XRD and ATR-FTIR) and PEGylated-PLGA polymers ( $^1\text{H}$  NMR and ATR-FTIR) were also reported in our previous publications (8-10, 29). In this study, IONs were fabricated by the thermal decomposition of iron-oleate precursor in the presence of an organic solvent with a high boiling point. Iron oxide nanoparticles, as shown in TEM image (Fig. 2a), had a narrow size distribution with an average particle size of  $8.6 \pm 0.9$  nm (Fig. 2b). Additionally, TEM image demonstrates the efficiency of the thermal decomposition method in producing monodispersed IONs. The PDI was calculated as 0.01, indicating that IONs were monodispersed. For biological applications, monodispersed IONs were coated with PEGylated-PLGA polymer by emulsion-sol-

vent evaporation method. The morphology and size of PEGylated-PLGA coated IONs were characterized via SEM/TEM analyses. According to SEM analysis (Fig. 2d), the PEGylated-PLGA-IONs exhibited spherical morphology with an average diameter of  $170 \pm 46$  nm (Fig. 2e). As shown in Fig. 2f, the IONs were uniformly distributed and clearly displayed in the PEGylated-PLGA matrix. Furthermore, the same image revealed that IONs in the core had a well-defined spherical shape, with no apparent particle aggregation. This situation may also assist the heating capacity (SAR) of PEGylated-PLGA-IONs in an alternating magnetic field.

The magnetic field-dependent magnetizations of the IONs and PEGylated-PLGA-IONs are shown in Fig. 2c. It is apparent that the magnetization curve has no hysteresis with zero coercivity and remanence, which indicates a superparamagnetic behavior. The saturation magnetization ( $M_s$ ) of IONs was 6 emu/g, which was lower than the values reported in the literature (30). However, the saturation magnetization of magnetic nanoparticles may change dramatically based on factors such as the particle size (31), the distortion of crystal symmetry (spin canting effect) (32), and whether or not the synthesis medium contains oxygen (27). On the other hand, the  $M_s$  of the PEGylated-PLGA-

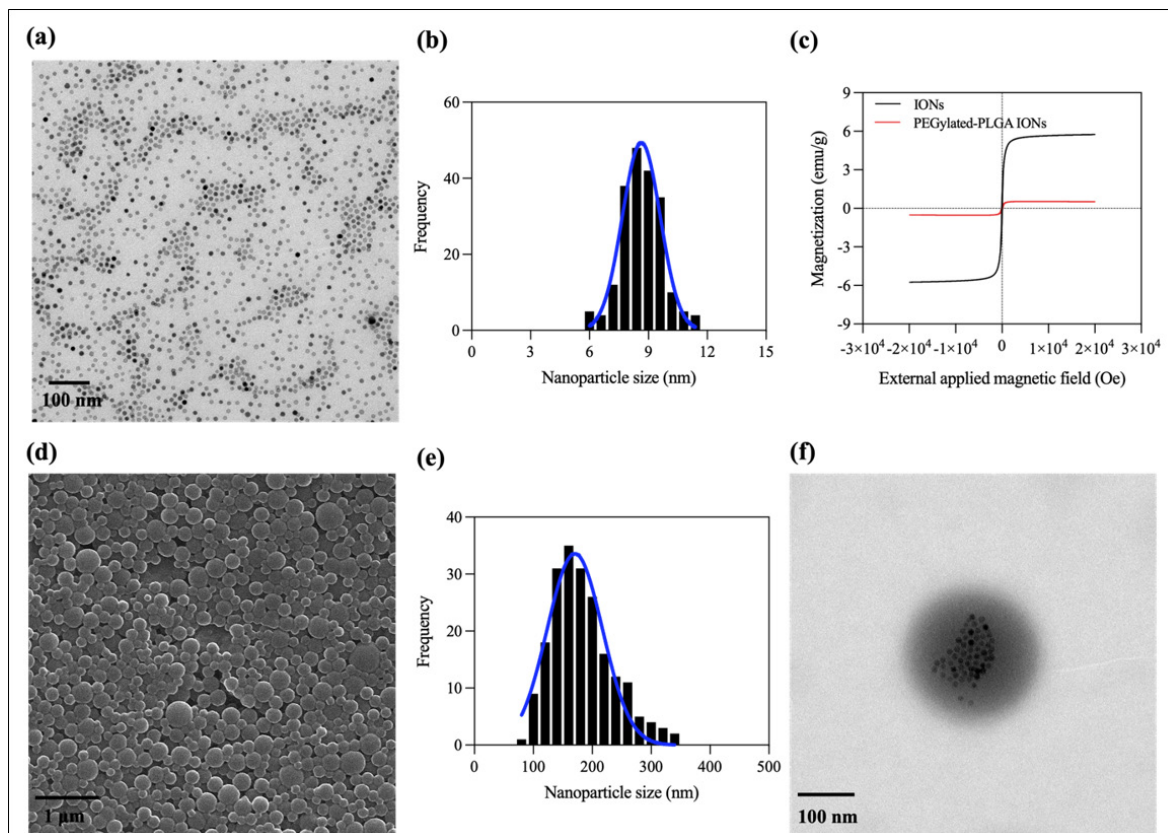


**Figure 2.** (a) The TEM image of monodisperse iron oxide nanoparticles (IONs), (b) size distribution histogram of IONs from TEM image, (c) hysteresis loops of IONs and PEGylated-PLGA coated IONs (PEGylated-PLGA-IONs), (d) SEM image of PEGylated-PLGA-IONs, (e) size distribution histogram of PEGylated-PLGA-IONs from SEM image, (f) TEM image of PEGylated-PLGA-IONs containing IONs homogeneously dispersed in the PEGylated-PLGA matrix.

IONS decreased to 0.6 emu/g. This reduction for PEGylated-PLGA-IONS is caused by the PEGylated-PLGA layers surrounding IONS. Although magnetization is a major factor in influencing IONS' heating efficiency, other factors, such as low aggregation, and homogeneous and uniform size distribution, are also crucial. Therefore, the hyperthermia efficiency of monodisperse and non-clustered IONS in the PEGylated-PLGA matrix (PEGylated-PLGA-IONS) was tested despite their low magnetization values.

### Induction heating performance of PEGylated-PLGA coated IONS

Before the induction heating experiments, the iron (Fe) concentration of the PEGylated-PLGA-IONS was measured using a colorimetric method (Fig. 3). For this reason, iron assay kit components were used to generate standard solutions with known iron concentrations. Next, a standard absorbance-total iron concentration curve was obtained (Fig. 3a), and it was used to determine iron content of the PEGylated-PLGA-IONS (Fig. 3b). The total Fe content was found to be 40 µg Fe/1 mg PEGylated-PLGA-IONS.

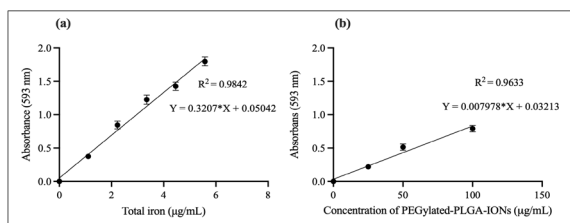


**Figure 3.** A colorimetric method to determine iron content with an iron assay kit components based on the instructions of the manufacturer, (a) total iron, (b) concentration of the PEGylated-PLGA coated IONS.

Afterward, PEGylated-PLGA-IONS were dispersed in distilled water (2.5 mL) at different concentrations (1.25, 2.5, 5, and 10 mg/mL). To induce heating, the PEGylated-PLGA-ION solutions are positioned in the coil's center, and an external alternating magnetic field (312 kHz, 100 A) is provided for 10 min. During the magnetic field exposure, the induced temperature of the solutions was measured and recorded in real-time (Fig. 4). According to the temperature profiles, the solution temperature increased by 9, 6, 2.1, and 1.5°C at the PEGylated-PLGA-IONS concentrations of 10, 5, 2.5, and 1.25 mg/mL, respectively (Fig. 4). However, SAR values of PEGylated-PLGA NPs (10, 5, 2.5 and 1.25 mg/mL) were found as 251.3, 313.4, 186.8 and 160.9 W/g, respectively (Table 1). The SAR value was maximum at 5 mg/mL nanoparticle concentration, while the highest temperature increase was observed at 10 mg/mL. On the other hand,  $\Delta T/\Delta t$  is the initial slope (0 to 30 s) for 1.25 mg/mL greater than 2.5 mg/mL. Even though the ION concentration is 50% lower than at 2.5 mg/mL, the SAR values are very close to those at 2.5 mg/mL. Therefore, it may be concluded that when an external field is applied, the aggregation rate of 2.5 mg/mL

or even the sedimentation rate is faster than 1.25 mg/mL. In other words, magnetic nanoparticles may exhibit larger SAR values at lower concentrations.

There are several studies in the literature on coating iron oxide nanoparticles with biocompatible materials to evaluate SAR values. For instance, albumin-stabilized carbon-encapsulated iron oxide nanoparticles (Fe@C-BSA) have been evaluated as a potential agent for magnetic nano hyperthermia. Among the tested concentrations of Fe@C-BSA (1, 2.5, and 5 mg/mL) for induction heating, the SAR value was determined to be the highest (437.64 W/g) at the lowest concentration (1 mg/mL) (33).

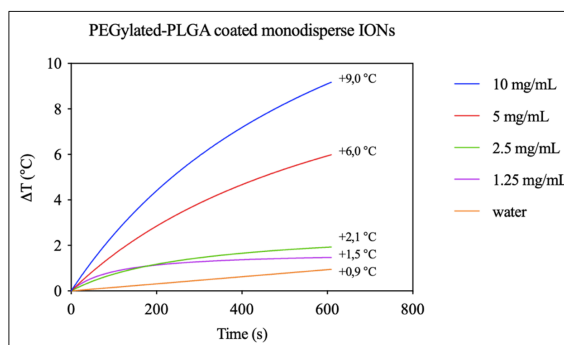


**Figure 4.** The time-dependent changes in the temperature of PEGylated-PLGA coated monodisperse iron oxide nanoparticles with different concentrations under the alternating magnetic field (100 A, 312 kHz, 10 min).

**Table 1.** Concentration-dependent specific absorption rate (SAR) of PEGylated-PLGA coated iron oxide nanoparticles (PEG-PLGA-IONS) in 2.5 mL of distilled water under an alternating magnetic field (312 kHz, 100 A, 10 min)

Concentration of PEG-PLGA-IONS (mg/mL)	Concentration of iron (Fe) in PEG-PLGA-IONS (according to colorimetric method using an iron assay kit) (µgFe/mL)	SAR (W/gFe)
10	250	251.3
5	125	313.4
2.5	62.5	186.8
1.25	31.25	160.9

In another study, hyperthermia efficacy and SAR value of magnetic graphene oxide-lignin nanocomposites (magnetic GO-lignin) were examined for cancer therapy. At the lower concentration of the nanocomposite (0.5 mg/mL), magnetic GO-lignin exhibits a higher specific absorption rate (121.22 W/g) (25). Therefore, a key factor influencing the specific absorption rate is the high stability and good homogeneity of magnetic nanocomposites in the aqueous phase. The SAR or corresponding parameters, specific loss power (SLP) or intrinsic loss power (ILP), can also be used to measure the magnetic heating efficacy of magnetic nanoparticles (34). Kim et al. report that the SLP of magnetic nanoparticles as a hyperthermia agent exhibited a strong

concentration-dependent oscillation behavior. Their finding suggests that the short interparticle distance, which is concentration related, may be the cause of decreasing SLP value (35). In light of these studies, determining the critical dose for a high-efficiency magnetic nano-hyperthermia agent is crucial for biomedical research. Moreover, it becomes clear that the monodisperse and non-aggregate distribution of iron oxide nanoparticles in the polymeric matrix has a significant impact on hyperthermia efficiency.

## CONCLUSION

The use of IONs in magnetic nano hyperthermia applications depends on their improvement with high heating efficacy, biocompatibility, and colloidal stability under physiological conditions. In this short study, PEGylated-PLGA coated monodisperse iron oxide nanoparticles were fabricated and tested as a potential magnetic nano hyperthermia agent. The results showed that highly monodisperse IONs ( $8.6 \pm 0.9$  nm) were clearly demonstrated with uniform distribution in the PEGylated-PLGA polymeric matrix. After that, different concentrations of PEGylated-PLGA coated monodisperse IONs were tested for their induction heating potentials. The highest SAR value was calculated to be 313 W/g at a nanoparticle concentration of 5 mg/mL, which included 125  $\mu\text{gFe/mL}$ . Therefore, these findings suggest that the monodisperse fabrication of IONs and their homogeneous distribution in the polymeric matrix may also contribute to the efficacy of hyperthermia on induction heating for cancer therapy.

## ACKNOWLEDGEMENTS

The author sincerely grateful for the assistance of the Cell and Tissue Engineering Research Group at Hacettepe University. The author also thankful to Dr. Mehmet Burak Kaynar for the hyperthermia measurements, as well as Dr. Soner Cakmak for all of the support.

## CONFLICT OF INTEREST

The authors declare that they have no known competing financial interests or personal relationships that could have appeared to influence the work reported in this paper.

## References

- Albarqi HA, Wong LH, Schumann C, Sabei FY, Korzun T, Li X, Hansen MN, Dhagat P, Moses AS, Taratula O, Taratula O. Biocompatible nanoclusters with high heating efficiency for systemically delivered magnetic hyperthermia. *ACS Nano*. 2019;13(6):6383-6395. doi:10.1021/acs.nano.8b06542.
- Senturk F, Cakmak S, Ozturk GG. Synthesis and characterization of oleic acid coated magnetic nanoparticles for hyperthermia applications. *Natural and Applied Sciences Journal*. 2019;2(2):16-29. doi:10.38061/idunas.657975.
- Beik J, Abed Z, Ghoreishi FS, Hosseini-Nami S, Mehrzadi S, Shakeri-Zadeh A, Kamrava SK. Nanotechnology in hyperthermia cancer therapy: From fundamental principles to advanced applications. *J Control Release*. 2016;235:205-221. doi:10.1016/j.jconrel.2016.05.062.
- Senturk F, Kocum IC, Guler Ozturk G. Stepwise implementation of a low-cost and portable radiofrequency hyperthermia system for in vitro/in vivo cancer studies. *Instrumentation Science & Technology*. 2021;1-13. doi:10.1080/10739149.2021.1927075.
- El-Boubbou K. Magnetic iron oxide nanoparticles as drug carriers: Preparation, conjugation and delivery. *Nanomedicine*. 2018;13(8):929-952. doi:10.2217/nnm-2017-0320.
- Deatsch AE, Evans BA. Heating efficiency in magnetic nanoparticle hyperthermia. *Journal of Magnetism and Magnetic Materials*. 2014;354:163-172. doi:10.1016/j.jmmm.2013.11.006.
- Senturk F. Current advances in glioblastoma therapy, in: N. Duran (Ed.), *Medical and health research theory, method and practice*. Livre De Lyon, Lyon. 2021;81:35-50.
- Senturk F, Cakmak S. Fabrication of curcumin-loaded magnetic PEGylated-PLGA nanocarriers tagged with GRGDS peptide for improving anticancer activity. *MethodsX*. 2023;10:2229. doi:10.1016/j.mex.2023.102229.
- Senturk F, Cakmak S, Kocum IC, Gumusderelioglu M, Ozturk GG. Effects of radiofrequency exposure on in vitro blood-brain barrier permeability in the presence of magnetic nanoparticles. *Biochem Biophys Res Commun*. 2022;597:91-97. doi: 10.1016/j.bbrc.2022.01.112.
- Senturk F, Cakmak S, Kocum IC, Gumusderelioglu M, Ozturk GG. GRGDS-conjugated and curcumin-loaded magnetic polymeric nanoparticles for the hyperthermia treatment of glioblastoma cells. *Colloids and Surfaces A: Physicochemical and Engineering Aspects*. 2021;126648. doi: 10.1016/j.colsurfa.2021.126648.
- Shubitidze F, Kekalo K, Stigliano R, Baker I. Magnetic nanoparticles with high specific absorption rate of electromagnetic energy at low field strength for hyperthermia therapy. *J Appl Phys*. 2015;117(9):094302. doi:10.1063/1.4907915.
- Xie L, Jin W, Chen H, Zhang Q. Superparamagnetic Iron Oxide Nanoparticles for Cancer Diagnosis and Therapy. *J Biomed Nanotechnol*. 2019;15(2):215-416. doi:10.1166/jbn.2019.2678
- Dadfar SM, Roemhild K, Drude NI, von Stillfried S, Knuchel R, Kiessling F, Lammers T. Iron oxide nanoparticles: Diagnostic, therapeutic and theranostic applications. *Adv Drug Deliv Rev*. 2019;138:302-325. doi:10.1016/j.addr.2019.01.005.
- Cai J, Miao YQ, Yu BZ, Ma P, Li L, Fan HM. Large-Scale, Facile Transfer of Oleic Acid-Stabilized Iron Oxide Nanoparticles to the Aqueous Phase for Biological Applications. *Langmuir*. 2017;33(7):1662-1669. doi:10.1021/acs.langmuir.6b03360.
- Aguilar AA, Ho MC, Chang E, Carlson KW, Natarajan A, Marciano T, Bomzon Ze, Patel CB. Permeabilizing cell membranes with electric fields. *Cancers (Basel)*. 2021;13(9):2283. doi:10.3390/cancers13092283.
- Senturk F, Bahadir A. Potential effects of electromagnetic fields used in cancer therapy on SARS-COV-2 infection. in A. Urfalioğlu and H. Kamalak (Eds.). *The clinical implications and evaluations of pandemic disease (COVID-19) in Turkey*. Livre De Lyon, Lyon 2021;78:1-18.
- Szasz A. Thermal and nonthermal effects of radiofrequency

- on living state and applications as an adjuvant with radiation therapy. *Journal of Radiation and Cancer Research*. 2019;10(1):1. doi:10.4103/jrcr.jrcr\_25\_18.
18. Park J, An K, Hwang Y, Park JG, Noh HJ, Kim JY, Park JH, Hwang NM, Hyeon T. Ultra-large-scale syntheses of monodisperse nanocrystals. *Nat Mater*. 2004;3(12):891-895. doi: 10.1038/nmat1251.
  19. Prabhu S, Goda JS, Mutalik S, Mohanty BS, Chaudhari P, Rai S, Udapa N, Rao BSS. A polymeric temozolomide nanocomposite against orthotopic glioblastoma xenograft: tumor-specific homing directed by nestin. *Nanoscale*. 2017;9(30):10919-10932. doi:10.1039/c7nr00305f.
  20. Chun SH, Shin SW, Amornkitbamrung L, Ahn SY, Yuk JS, Sim SJ, Luo D, Um SH. Polymeric Nanocomplex Encapsulating Iron Oxide Nanoparticles in Constant Size for Controllable Magnetic Field Reactivity. *Langmuir*. 2018;34(43):12827-33.
  21. Raval N, Maheshwari R, Kalyane D, Youngren-Ortiz SR, Chougule MB, Tekade RK. Importance of physicochemical characterization of nanoparticles in pharmaceutical product development. *Basic fundamentals of drug delivery*. 2019:369-400. doi:10.1016/B978-0-12-817909-3.00010-8.
  22. Ghosh R, Pradhan L, Devi YP, Meena SS, Tewari R, Kumar A, Sharma S, Gajbhiye NS, Vatsa RK, Pandey BN, Ningthoujam RS. Induction heating studies of Fe<sub>3</sub>O<sub>4</sub> magnetic nanoparticles capped with oleic acid and polyethylene glycol for hyperthermia. *J Mater Chem*. 2011;21(35). doi:10.1039/c1jm10092k.
  23. Wildeboer R, Southern P, Pankhurst Q. On the reliable measurement of specific absorption rates and intrinsic loss parameters in magnetic hyperthermia materials. *Journal of Physics D: Applied Physics*. 2014;47(49):495003. doi:10.1088/0022-3727/47/49/495003.
  24. Ruggiero MR, Geninatti Crich S, Sieni E, Sgarbossa P, Cavallari E, Stefania R, Dughiero F, Aime S. Iron oxide/PLGA nanoparticles for magnetically controlled drug release. *International Journal of Applied Electromagnetics and Mechanics*. 2017;53(S1):S53-S60. doi:10.3233/JAE-162246.
  25. Eivazzadeh-Keihan R, Asgharinasl S, Aliabadi HAM, Tahmasebi B, Radinekiyan F, Maleki A, Bahreinizad H, Mahdavi M, Alavijeh MS, Saber R. Magnetic graphene oxide–lignin nanobiocomposite: a novel, eco-friendly and stable nanostructure suitable for hyperthermia in cancer therapy. *RSC advances*. 2022;12(6):3593-3601. doi:10.1039/D1RA08640E.
  26. Kossatz S, Ludwig R, Dähring H, Ettl V, Rimkus G, Marciello M, Salas G, Patel V, Teran FJ, Hilger I. High therapeutic efficiency of magnetic hyperthermia in xenograft models achieved with moderate temperature dosages in the tumor area. *Pharm Res*. 2014;31(12):3274-88. doi:10.1007/s11095-014-1417-0
  27. Unni M, Uhl AM, Saviwala S, Savitzky BH, Dhavalikar R, Garraud N, Arnold DP, Kourkoutis LF, Andrew JS, Rinaldi C. Thermal Decomposition Synthesis of Iron Oxide Nanoparticles with Diminished Magnetic Dead Layer by Controlled Addition of Oxygen. *ACS Nano*. 2017;11(2):2284-303. doi:10.1021/acsnano.7b00609.
  28. Dallet L, Stanicki D, Voisin P, Miraux S, Ribot EJ. Micron-sized iron oxide particles for both MRI cell tracking and magnetic fluid hyperthermia treatment. *Sci Rep*. 2021;11(1):1-13. doi:10.1038/s41598-021-82095-6.
  29. Senturk F, Cakmak S, Gumusderelioglu M, Ozturk GG. Hydrolytic instability and low-loading levels of temozolomide to magnetic PLGA nanoparticles remain challenging against glioblastoma therapy. *Journal of Drug Delivery Science and Technology*. 2022;68:103101. doi:10.1016/j.jddst.2022.103101.
  30. Spivakov A, Lin C-R, Chang Y-C, Wang C-C, Sarychev D. Magnetic and Magneto-Optical Properties of Iron Oxides Nanoparticles Synthesized under Atmospheric Pressure. *Nanomaterials*. 2020;10(9):1888. doi:10.3390/nano10091888
  31. Smolensky ED, Park H-YE, Zhou Y, Rolla GA, Marjańska M, Botta M, Pierre VC. Scaling laws at the nanosize: the effect of particle size and shape on the magnetism and relaxivity of iron oxide nanoparticle contrast agents. *Journal of Materials Chemistry B*. 2013;1(22):2818-28. doi:10.1039/C3TB00369H.
  32. Wu K, Su D, Liu J, Saha R, Wang J-P. Magnetic nanoparticles in nanomedicine: A review of recent advances. *Nanotechnology*. 2019;30(50):502003. doi:10.1088/1361-6528/ab4241.
  33. Ramírez-Morales MA, Goldt AE, Kalachikova PM, Ramirez B JA, Suzuki M, Zhigach AN, Ben Salah A, Shurygina LI, Shandakov SD, Zatsepina T. Albumin stabilized Fe@ C core-shell nanoparticles as candidates for magnetic hyperthermia therapy. *Nanomaterials*. 2022;12(16):2869. doi:10.3390/nano12162869.
  34. Liu X, Zhang Y, Wang Y, Zhu W, Li G, Ma X, Zhang Y, Chen S, Tiwari S, Shi K. Comprehensive understanding of magnetic hyperthermia for improving antitumor therapeutic efficacy. *Theranostics*. 2020;10(8):3793. doi:10.7150/thno.40805.
  35. Kim J-w, Wang J, Kim H, Bae S. Concentration-dependent oscillation of specific loss power in magnetic nanofluid hyperthermia. *Sci Rep*. 2021;11(1):1-10. doi:10.1038/s41598-020-79871-1.